

Single-pulse coherent anti-Stokes Raman spectroscopy in the fingerprint spectral region

Nirit Dudovich, Dan Oron, and Yaron Silberberg

Department of Physics of Complex Systems, Weizmann Institute of Science, Rehovot 76100, Israel

(Received 27 January 2003; accepted 25 February 2003)

Quantum coherent control techniques are applied to achieve high spectral resolution nonlinear vibrational spectroscopy using a single ultrashort laser source. By controlling the spectral phase of ~ 10 fs pulses, we are able to obtain detailed coherent anti-Stokes Raman (CARS) spectra in the important fingerprint spectral region, which reflects the structural chemical information. A full theoretical analysis and an experimental demonstration of two alternative schemes leading to spectral resolution two orders of magnitude better than the pulse bandwidth are presented. The first involves selective excitation of vibrational levels within the pulse bandwidth by periodic modulation of the spectral phase of the pulse. In the second scheme an effective narrow probing of the vibrational level has been achieved by phase shifting of a narrow spectral band. Single-pulse CARS offers an attractive alternative to conventional multibeam nonlinear vibrational spectroscopy techniques. © 2003 American Institute of Physics. [DOI: 10.1063/1.1568072]

I. INTRODUCTION

Quantum coherent control has been a subject of extensive research in recent years. The primary goal in this field is to direct a quantum system to a specific final state, usually by means of its interaction with light. Following the recent development of femtosecond lasers, this capability has been proposed and demonstrated in a variety of atomic, molecular, and solid-state systems. Control of a two photon transition process, the most basic nonlinear effect, has been first demonstrated by Weiner *et al.*¹ for stimulated Raman processes, and later by our group for two photon absorption (TPA) processes.²⁻⁴ It was demonstrated that by tailoring the temporal shape of the pulse the transition rate can be either annihilated or maximized. Control over more complicated systems often involves the use of adaptive techniques,⁵ in which the spectral phase is determined by a feedback optimization procedure. This approach has been applied to a variety of systems, such as selective chemical bond breaking,⁶ high-harmonic generation,⁷ and controlling the shape of a quantum wave function.⁸ The present work deals with the application of coherent control to spectroscopy, and in particular, to coherent anti-Stokes Raman spectroscopy (CARS). We demonstrate several different schemes to achieve CARS with a single short pulse source using coherent control techniques, and we show that these ideas can be implemented in the important spectral range known as the fingerprint region.

CARS is a spectroscopic tool for the investigation of vibrational and rotational levels in molecules.⁹ In a CARS process, a pump and a Stokes photons with frequencies ω_p and ω_s coherently excite a vibrational level at an energy $\hbar(\omega_p - \omega_s)$. A probe photon at ω_{pr} interacts with the excited level to emit a signal photon at the frequency $(\omega_p + \omega_{pr} - \omega_s)$. The energy level diagram of this process is illustrated in Fig. 1(a). Typically, two narrow-band (narrower than the typical linewidth of Raman levels, corresponding to picosecond pulses) beams are used, exciting only Raman levels in resonance with their energy difference (generally, in this case

$\omega_p = \omega_{pr}$). In time-resolved CARS scheme the two exciting pulses have a larger bandwidth, thus simultaneously populating several Raman levels. The spectral data is obtained by measuring the interference pattern of the CARS signal from a third, delayed probe pulse.¹⁰ When using a narrow-band pump and a broadband Stokes beams, simultaneous measurement of an entire band of the Raman spectrum can be performed (multiplex CARS).⁹ Recently, an alternative approach to time-resolved CARS, where spectral resolution an order of magnitude better than the pulse bandwidth is achieved by means of coherent control of either the pump and Stokes beams¹¹ or the probe beam,¹² has been demonstrated.

When the pulse duration is shorter than the vibrational period of the molecule, the excitation can be induced within a single pulse, followed by a delayed probe, in a mechanism called impulsive stimulated Raman scattering (ISRS).^{1,13} Our group has recently presented a new approach, single pulse CARS spectroscopy, by using coherent control techniques. In this case both the excitation and the probing are conducted by the same pulse.¹⁴ The CARS signal is thus produced by an intrapulse four-wave mixing process. Each of the different spectral components of the signal results from the interference of all the quantum paths that contribute to the nonlinear polarization. However, inducing the process with a single transform limited ultrashort pulse results in several inherent difficulties. The major difficulty arises from the fact that all vibrational levels with energies within the pulse bandwidth are excited. As a result the spectral resolution of this process is limited by the pulse bandwidth. Another difficulty results from the large nonresonant background. As the pulse duration is decreased, the nonresonant background intensity increases much more rapidly than that of the resonant signal.¹⁵ A third difficulty, of a more technical nature, arises from the partial spectral overlap between the excitation pulse and the CARS signal, which is orders of magnitude weaker. This is overcome by partial blocking of the excitation pulse spec-

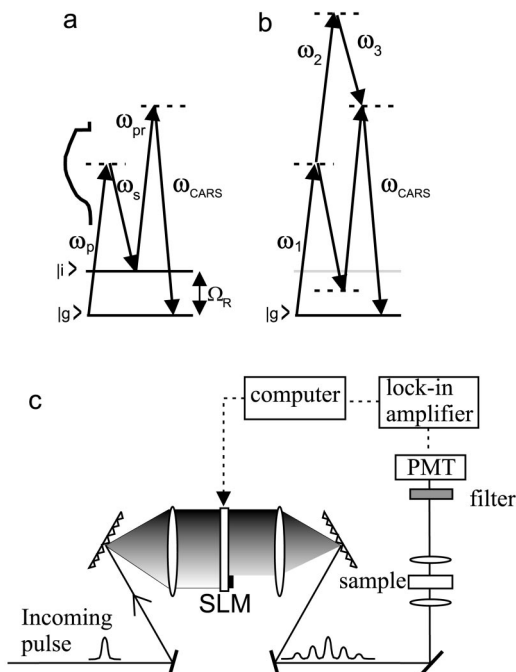


FIG. 1. Schematic description of the different mechanisms that can contribute to the measured CARS signal and the experimental setup. (a) Energy level scheme of the single pulse resonant CARS process. The pulse spectrum, blocked at its high energy end, has a bandwidth larger than the vibrational energy level. (b) Energy level scheme of the nonresonant CARS process. (c) Diagram of the experimental setup.

trum and proper spectral filtering of the measured signal.

These difficulties can, however, be overcome by the implementation of coherent control techniques. We have recently demonstrated how coherent control can be applied both to restore the high spectral resolution and to increase the ratio of the resonant signal and the nonresonant background. Using several schemes we were able to perform single-pulse spectroscopy in the energy range of $400\text{--}800\text{ cm}^{-1}$, using pulses with a 70 nm (1100 cm^{-1}) spectral bandwidth. One scheme involves selective excitation of vibrational levels within the pulse bandwidth.¹⁴ In an alternative approach, single pulse multiplex CARS has been demonstrated.¹⁶ In this scheme an effective narrow probing of the vibrational level has been achieved by phase shifting of a narrow spectral band. In yet another approach, polarization pulse shaping has been applied to split the short pulse into a broadband pump and a narrow-band orthogonally polarized probe.¹⁷ Most organic molecules, however, have unique vibrational spectra primarily in the $1000\text{--}1500\text{ cm}^{-1}$ range, known as the fingerprint spectral region. In order to induce a single pulse CARS process in this region, pulses of a duration of $10\text{--}15\text{ fs}$ are required. However, shortening the pulse duration further increases the difficulties involved with both spectral resolution and the nonresonant background. Stretching the capabilities of the pulse shaping techniques, and using a state-of-the-art pulse shaper,¹⁸ enabling a high degree of control over pulses with a spectral bandwidth of over 2000 cm^{-1} , we achieve high resolution single-pulse CARS in the fingerprint region. Two alternative schemes leading to spectral resolution two orders of magnitude better than the pulse bandwidth are presented in the following sec-

tions. We begin by presenting a detailed theoretical analysis of the CARS process in Sec. II. The first scheme, involving selective excitation of the various Raman levels, is demonstrated in Sec. III, while the second, inducing narrow spectral probing of the Raman level populations is demonstrated in Sec. IV. A summary and conclusions are given in Sec. V.

II. THEORETICAL ANALYSIS

Consider a CARS process induced by a single ultrashort pulse whose electric field envelope is given by $E(t)$. The high frequency edge of the excitation pulse spectrum is blocked at ω_{\max} and the signal is measured at $\omega > (\omega_{\max} + \epsilon)$ (where ϵ is determined by the resolution of the spectral filter). The third order signal can be generated by two different processes as described in Figs. 1(a)–1(b). The first process, described in Fig. 1(a), is a resonant CARS process, in which an intermediate vibrational level is excited by the pulse. To generate a CARS signal, the excitation should be probed, within the decoherence time of the vibrational level.

The second process described in Fig. 1(b), is a nonresonant one, usually known as self phase modulation (SPM). In this process the third order polarization is generated instantaneously, since all the intermediate levels are considerably distant from the pulse frequency. While a truly instantaneous SPM process should exhibit a flat spectral response, the measured nonresonant spectrum indicates that the nonresonant response is not entirely flat. Fitting the measured spectrum, the nonresonant response has a decoherence time which is roughly similar to the pulse duration.

The temporal third order polarization driving the CARS signal induced by a single pulse with electric field envelope $E(t)$ is predicted by third order time dependent perturbation theory,

$$P^{(3)}(t) = -\frac{i}{\hbar^3} \sum_{nfm} \mu_{fm} \mu_{mg} \mu_{gn} \mu_{nf} \exp(-i(\omega_{gm} + \Gamma_{gm})t) \times \int_{-\infty}^t dt_1 \int_{-\infty}^{t_1} dt_2 \int_{-\infty}^{t_2} dt_3 \quad (1)$$

$$E(t_3)E^*(t_2)E(t_1) \times \exp(i(\omega_{fm} + \Gamma_{fm})t_1) \times \exp(i(\omega_{nf} + \Gamma_{nf})t_2) \exp(i(\omega_{gn} + \Gamma_{gn})t_3),$$

where $|g\rangle$ is the ground level, $|n\rangle$, $|f\rangle$, and $|m\rangle$ the intermediate levels, μ_{ij} the dipole moments, $\omega_{ij} = (E_i - E_j)/\hbar$, Γ_{ij} the linewidths, and the summation is performed over all possible intermediate states of the unperturbed molecule. The polarization spectrum is obtained by transforming Eq. (1) to the frequency domain,

$$P^{(3)}(\omega) = -\frac{1}{\hbar^3} \sum_{nfm} \mu_{fm} \mu_{mg} \mu_{gn} \mu_{nf} \frac{1}{\omega - \omega_{mg} - i\Gamma_3} \times \int_0^\infty d\Omega \frac{1}{\Omega - \omega_{fg} - i\Gamma_2} E(\omega - \Omega) \times \int_0^\infty d\omega' \frac{1}{\omega' - \omega_{ng} - i\Gamma_1} E^*(\omega')E(\Omega + \omega'), \quad (2)$$

where $E(\omega) = |E(\omega)| \exp(i\phi(\omega))$ is the Fourier transform of $E(t)$, $\Gamma_1 = \Gamma_{gn}$, $\Gamma_2 = \Gamma_{gn} + \Gamma_{nf}$, $\Gamma_3 = \Gamma_{gn} + \Gamma_{nf} + \Gamma_{fm}$.

Assuming that both $|\omega - \omega_{ng}| \gg \Delta\omega$ and $|\omega - \omega_{mg}| \gg \Delta\omega$, where $\Delta\omega$ is the pulse spectral bandwidth (i.e., no electronic resonance), Eq. (2) can be approximated by

$$P^{(3)}(\omega) = -\frac{1}{\hbar^3} \sum_{nfm} \mu_{fm} \mu_{mg} \mu_{gn} \mu_{nf} \times \frac{1}{(\omega_0 - \omega_{ng})(\omega_0 - \omega_{mg})} \times \int_0^\infty d\Omega \frac{1}{\Omega - \omega_{fg} - i\Gamma_2} E(\omega - \Omega) \times \int_0^\infty d\omega' E^*(\omega') E(\Omega + \omega'), \quad (3)$$

where ω_0 is the central frequency of the pulse spectrum. According to Eq. (3), we can approximate the polarization spectrum of the different processes. A resonant CARS process is described by

$$P_r^{(3)}(\omega) = C_r \int_0^\infty d\Omega \frac{1}{\Omega - \Omega_R - i\Gamma_R} E(\omega - \Omega) A(\Omega). \quad (4)$$

Here $A(\Omega)$ is the probability amplitude to populate a vibrational level with energy Ω , which is a sum of all possible two-photon pairs leading to the same intermediate state,

$$A(\Omega) = \int_0^\infty d\omega' E^*(\omega') E(\Omega + \omega'). \quad (5)$$

Ω_R and Γ_R are the Raman level frequency and linewidth, respectively, and C_r is a constant which includes the summation over the dipole moments. $E(\omega - \Omega)$ in Eq. (4) is the probe field.

Similarly, the nonresonant CARS process can be approximated as

$$P_{nr}^{(3)}(\omega) = C_{nr} \int_0^\infty d\Omega \frac{1}{\Omega} E(\omega - \Omega) A(\Omega), \quad (6)$$

where the $1/\Omega$ term is a correction term accounting for the not fully instantaneous nature of the process. This results in good agreement with the measured nonresonant CARS spectrum.

III. SPECTROSCOPY BY SELECTIVE EXCITATION

A. Theoretical analysis

The population amplitude $A(\Omega)$ is determined by the interference between all frequency pairs within the excitation pulse separated by Ω . The highest energy level that can be excited by a single pulse is limited by its spectral span. The contribution of the different pairs interferes with a relative phase of $\phi(\omega) - \phi(\omega - \Omega)$. Thus, constructive interference is achieved when $\phi(\omega) = \phi(\omega - \Omega)$ for all frequency components. This clearly holds for all values of Ω for excitation with a transform limited pulse, as all frequency components have the same phase. When the spectral phase is modulated periodically with a period Ω_m , constructive interference is

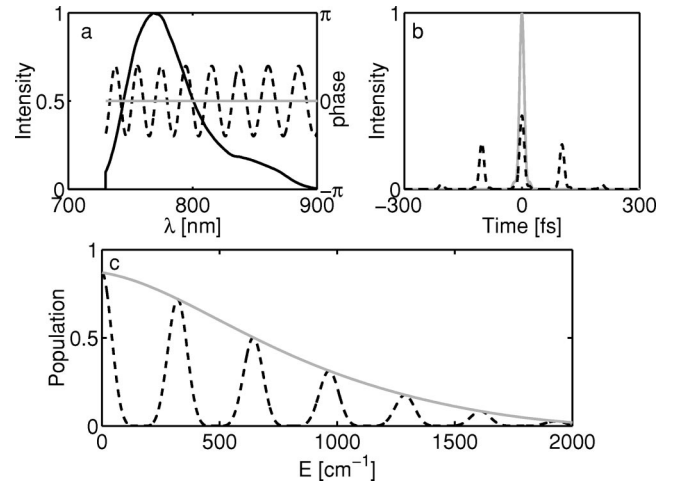


FIG. 2. (a) Schematic drawing of the excitation pulse spectral intensity (solid black line) with the spectral phase of a transform limited pulse (gray line) and a modulated phase shaped pulse (dashed line). (b) Temporal intensity of a transform limited pulse (gray line) and a modulated phase shaped pulse (dashed line). (c) Calculated population amplitude $A(\Omega)$ for transform limited pulse (gray line) and the shaped pulse (dashed line).

achieved only for $\Omega = N\Omega_m$ (N integer). Figures 2(a)–2(c) illustrate the effect of periodic modulation of the spectral phase on the temporal shape of the pulse and on $A(\Omega)$. Figure 2(a) depicts the power spectrum of the pulse, blocked at 730 nm, which is the one used in the experiments described in the following sections. Note that although the full-width at half maximum (FWHM) of the pulse is only 60 nm, the spectrum is clearly not Gaussian, so the effective bandwidth is about 140 nm. Two cases, of either a uniform or a modulated spectral phase, are considered. Figure 2(b) shows both the transform limited (uniform phase) and the shaped pulse in the time domain. As is evident from Fig. 2(b), a periodic spectral phase is equivalent to splitting the pulse in time domain to several equally spaced pulses, each delayed by $\tau_m = 2\pi/\Omega_m$. This pulse train is able to resonantly excite only vibrations with a period $T = \tau_m/N$ (N integer). The population amplitude $A(\Omega)$, described in Fig. 2(c), decays monotonically with the vibration energy for the transform limited case. For a modulated phase function, oscillations appear in $A(\Omega)$; only frequencies that fulfill $\Omega = N\Omega_m$ reach the excitation amplitude of a transform limited pulse.

The final CARS signal depends on the population amplitude, but also on the phase modulation of the probe spectrum as is evident from Eqs. (4) and (6). According to Eq. (4) the resonant CARS process can be expressed as

$$P_r^{(3)}(\omega) \approx C_r \left[i\pi E(\omega - \Omega_R) A(\Omega_R) + \oint_0^\infty d\Omega \times \frac{\Omega - \Omega_R}{(\Omega - \Omega_R)^2 + \Gamma_R^2} E(\omega - \Omega) A(\Omega) \right], \quad (7)$$

where \oint is the principal value of Cauchy. The first term corresponds to the on-resonant contribution, and the second term is an integration over the contribution of the off-resonant spectral components. The resonant signal thus has a narrow response around $\Omega = \Omega_R$. The weight function of the

integrand of the second term inverts its sign around the resonance, therefore the total contribution of the integral depends on the symmetry of $E(\omega - \Omega)A(\Omega)$ around $\Omega = \Omega_R$. In the transform limited case both $A(\Omega)$ and $E(\omega - \Omega)$ are nearly symmetric for all values of Ω . Therefore the contribution of the off-resonant term is negligible. The polarization spectrum can be approximated in this case by $P_r^{(3)}(\omega) \approx i\pi CE(\omega - \Omega_R)A(\Omega_R)$, which is a replica of the pulse spectrum shifted by Ω_R . Spectral phase manipulation will change the symmetry of $E(\omega - \Omega)A(\Omega)$ for different values ω and will therefore induce variations in the polarization spectrum.

The influence of a modulated spectral phase function on the resonant CARS spectrum can be easily understood in the time domain. Since each pulse in the train serves also as a probe, a train of CARS signal pulses is induced. If the pulses are separated by an integer number of the vibrational periods, the excited population is coherently accumulated. The resonant CARS signal is thus comprised of a train of pulses with increasing intensity, resulting in a modulated spectrum. However, when this modulation frequency significantly exceeds $2\pi/\Delta\omega$, the total signal intensity averages over several periods and the measured intensity is proportional to $|A(\Omega_R)|^2$. Thus, with a proper choice of the phase function periodicity, the resonant signal reaches its transform limited value.

The nonresonant process is (nearly) instantaneous and therefore is induced by each of the pulses in the train separately. A similar train of the nonresonant signal is induced, resulting, again, in a modulated spectrum. As in the resonant case, when the modulation frequency significantly exceeds $2\pi/\Delta\omega$ this is averaged out and the measured intensity is proportional to $|\int_{\epsilon}^{\epsilon+\Delta\omega} (d\Omega/\Omega)A(\Omega)|^2$. In contrast with the resonant process, this intensity is significantly lower than that generated by a transform limited pulse regardless of the phase function periodicity.

The total measured signal is the interference of the signals generated by the two different processes. In the common case where the nonresonant background is considerably larger than the resonant signal, the resonant signal is measured by a "heterodyne detection" with it to yield

$$\begin{aligned} |P(\omega)^{(3)}|^2 &= |P(\omega)_r^{(3)} + P(\omega)_{nr}^{(3)}|^2 \\ &\approx |P(\omega)_{nr}^{(3)}|^2 + 2 \operatorname{Re}[P(\omega)_r^{(3)}P(\omega)_{nr}^{(3)*}]. \end{aligned} \quad (8)$$

By exploiting the different spectral response of the resonant and nonresonant components, it is possible to significantly reduce the nonresonant background while maintaining the resonant signal.

B. Experimental results

We demonstrate selective excitation of a single-pulse resonant CARS process in the fingerprint region in several molecules. The measurable Raman energy range of our system is about 700–1400 cm^{-1} , which covers most of the fingerprint region. The lower limit of this range is adjusted by setting the spectral blocker in the pulse shaper [see Fig. 1(c)]. Limiting the range to one octave simplifies the analysis of the results, as will be evident below. The upper bound is dictated by the limited spectral content of the excitation

pulse. The ultrashort pulses were produced by a Ti:sapphire laser emitting 14 fs FWHM transform limited pulses, having a longer pedestal of about 40 fs. We adjusted the spectral phase of the pulse with a programmable pulse shaper, which includes a 640 pixel liquid crystal spatial light modulator (SLM) at its Fourier plane.^{18,19} The spectral resolution, determined by the spot size at the Fourier plane is 0.3 nm (equivalent to about 5 cm^{-1}). The high energy end is blocked at 730 nm. A spectral band between 730 and 870 nm, corresponding to an energy span of 2100 cm^{-1} , is used to induce the CARS process. The shaper was used both for correction of dispersion as well as for the application of any additional desired spectral phase function. The shaped pulses are focused into the sample using a $NA = 0.2$ objective. The CARS signal is filtered out by a sharp-cut shortpass filter at 720 nm (Omega optical) and measured with a photomultiplier tube and a lock-in amplifier. Note that in this scheme the entire CARS signal is collected, and we do not attempt to resolve it spectrally. An outline of the experimental setup is shown in Fig. 1(c).

We applied a modulated phase function of the form $\phi(\omega) = 1.25 \cos[\tau_m(\omega - \omega_0)]$,²⁰ holding the phase fixed at $\lambda_0 = 760 \text{ nm}$. As discussed above, this spectral phase leads to a train of temporal pulses separated by τ_m , which was varied from 400 to 1000 fs. Figure 3(a) shows the CARS signal generated in a $\text{Ba}(\text{NO}_3)_2$ crystal, which has a single vibrational resonance at 1048 cm^{-1} . The signal oscillates as the delay between the pulses increases, reaching a peak each time τ_m is commensurate with the vibrational period. Fourier analysis of these oscillations retrieves the level energy, as seen in Fig. 3(b). A similar measurement in diamond, which has a higher resonant level at 1333 cm^{-1} , gives more rapid oscillations, corresponding to a sharp peak close to the upper spectral limit of our system [see Figs. 3(c)–3(d)]. When the molecule has more than one resonant level, as in toluene (which has two strong resonances at 788 cm^{-1} and 1028 cm^{-1}) beats are observed in the signal, and additional peaks are observed in the Fourier transform [see Figs. 3(e)–3(f)]. When measuring the signal from a material having a complex Raman spectrum, a complicated interference pattern is observed. The detailed spectrum of a complex polymer such as lexan (bisphenol A polycarbonate) can still be extracted, however, with good accuracy [see Figs. 3(g)–3(h)]. The spectral resolution of the Fourier transform operation is about 70 times better than the effective pulse bandwidth, i.e., about 30 cm^{-1} . The resolution is determined by the smallest period of phase modulation that can be applied, which is limited by the number of pixels on the SLM.

Spectral resolution is optimized by use of a simple sinusoidal phase function. By applying a sinusoidal phase function, however, the input pulse is split into a rather short train of pulses. The nonresonant background, which depends directly on the pulse peak intensity, can be further reduced by splitting the single pulse into a longer train, containing a larger number of weaker pulses. This can be achieved by adding higher harmonic orders to the applied phase functions. This phase function can be expressed as a sum of higher harmonic orders, $\phi(\omega) = \sum_n F_n \cos(n\tau_m(\omega - \omega_0))$, where F_n are the corresponding weights. In Fig. 4(a) we

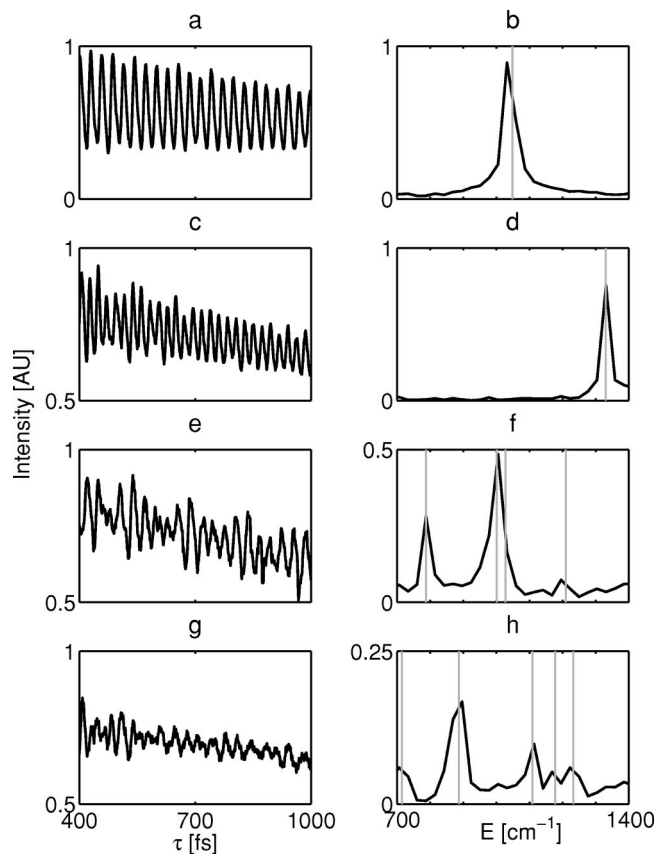


FIG. 3. Selective excitation of vibrational levels in various materials using a modulated spectral phase function. The CARS signal intensity as a function of the time separation between the different pulses in the pulse train (left column) and the extracted Raman spectra, derived by Fourier transformation of the intensity curves (right column) are given for (a)–(b) $\text{Ba}(\text{NO}_3)_2$ (resonant at 1048 cm^{-1}), (c)–(d) diamond (resonant at 1333 cm^{-1}), (e)–(f) toluene (resonant at 788 , 1001 , 1028 , and 1210 cm^{-1}), and (g)–(h) lexan (resonant at 704 , 887 , 1109 , 1178 , and 1232 cm^{-1}).

show the reduction of the nonresonant signal when the number of harmonics of the phase function is increased. When using a phase function containing just two harmonics the nonresonant signal is attenuated by a factor of ~ 80 , while increasing the number of harmonics to four reduces it by a factor of ~ 250 . At the same time, the resonant signal is hardly affected, as is evident from Fig. 4(b), showing this measurement in $\text{Ba}(\text{NO}_3)_2$. The signal measured with four harmonics is predominantly a resonant one, with a negligible contribution from the nonresonant background. The maximal reduction depends on the number of the different harmonics on the SLM, and is limited again by the pixellization of the the SLM. Such phase functions should be applied when attempting to detect specific Raman levels of molecules with a known level structure.

IV. SPECTROSCOPY BY NARROW PROBING

A. Theoretical analysis

The previous section demonstrates coherent control of the CARS process via manipulation of $A(\Omega)$. We exploited the interferences between all the different two-photon paths which populate a given vibrational energy level. Furthermore, by reducing the peak intensity of the pulse we reduced

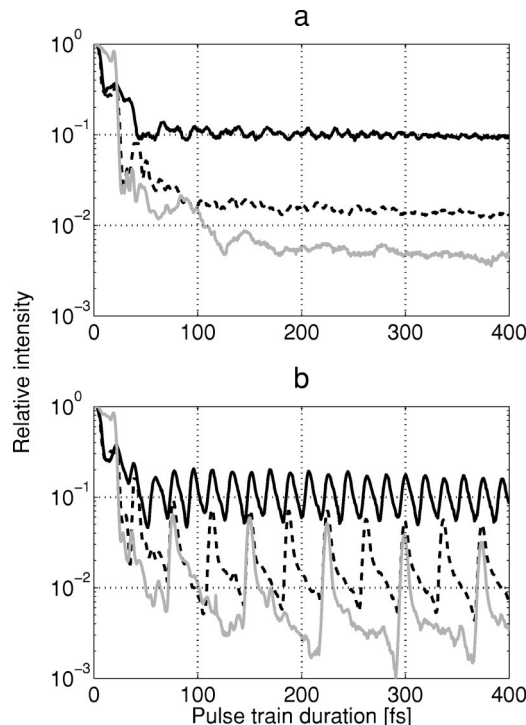


FIG. 4. Background suppression using periodic spectral phase functions with additional harmonic orders. The CARS intensity is shown as a function of the total pulse train duration for a sinusoidal phase function ($F_1=1.25$, solid line), a phase function containing two harmonics ($F_1=1.3$, $F_2=-1.7$, dashed line) and four harmonics ($F_1=-0.8$, $F_2=0.5$, $F_3=1.4$, $F_4=-1.5$, gray line). The measured results are for (a) glass (nonresonant) and (b) $\text{Ba}(\text{NO}_3)_2$ (resonant at 1048 cm^{-1}).

the nonresonant background by over two orders of magnitude. A different approach, where instead of reducing the nonresonant background it is used as a local oscillator for phase-sensitive detection of the resonant signal, has been recently demonstrated.¹⁶ In this scheme the loss of selectivity due to the large bandwidth of the excitation pulse is overcome by analyzing the spectrum of the signal that is induced by spectrally narrow probing.

As is evident from the second term in Eq. (7), the CARS signal at frequency ω is generated by all quantum paths which pass in the vicinity of the resonance. As discussed above, a transform limited pulse induces destructive interference between the different paths, due to the symmetry of $E(\omega-\Omega)A(\Omega)$ about the resonance. By applying a π phase shift around $E(\omega-\Omega)$, constructive interference is induced, resulting in a sharp peak in the resonant CARS spectrum. This effect was first demonstrated in a three-color CARS experiment by Oron *et al.*,¹² where shaping the probe beam enhanced the spectral resolution of the CARS process by an order of magnitude. However, since the process is induced by a single pulse, such a phase manipulation will also affect the population amplitude. The change in the population amplitude is minimized by applying a phase shift only to a narrow spectral band. Figures 5(a)–5(c) illustrate the effect of such a π phase gate on the temporal shape of the pulse and on the population amplitude. As evident, the narrow π phase gate hardly affects the pulse, merely reducing the peak intensity by about 20%. As a result, the population amplitude

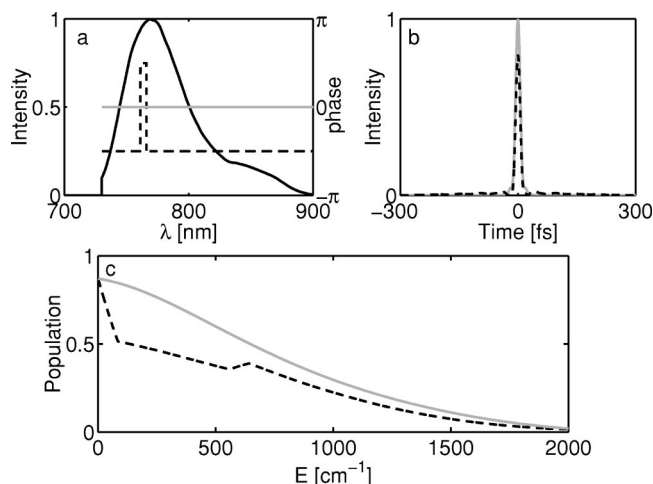


FIG. 5. Schematic drawing of the excitation pulse spectral intensity (solid black line) and spectral phase of a transform limited pulse (gray line) and a 10-pixel π phase gate pulse (dashed line). (b) Temporal intensity of a transform limited pulse (gray line) and a π phase gate shaped pulse (dashed line). (c) Calculated population amplitude $A(\Omega)$ for the transform limited pulse (gray line) and the shaped pulse (dashed line).

$A(\Omega)$, described in Fig. 5(c), is somewhat reduced but still varies slowly in the measured energy range. Phase manipulation, however, does not only induce enhancement of the resonant signal, but also affects the relative phase between it and the nonresonant background. The resonant polarization spectrum at the phase gates edges shifted by Raman energy can be approximated to be⁴

$$P_r^{(3)}(\omega_{\text{right}}^{\text{left}} + \Omega_R) \approx \pm \frac{1}{\pi} C_r \ln \left(\frac{\Delta_g}{\Gamma_R} \right) E(\omega_{\text{right}}^{\text{left}}) A(\Omega_R), \quad (9)$$

where $\omega_{\text{right}}^{\text{left}}$ are the left and right edges of the phase gate and Δ_g its width. The relative phase between the resonant signal and the nonresonant background thus changes from 0 to π across the phase gate (shifted by the Raman energy). These phase variations affect the total spectrum of the CARS signal in a rather dramatic manner. In the case of a transform limited pulse the resonant and the nonresonant signals are in quadrature. Since the nonresonant signal is typically much larger than the resonant one, intensity variations of the CARS spectrum depend on the resonant signal to second order. However by changing the relative phase between the two signals, a stronger interference pattern between the two can be induced, where the effect of the weak resonant signal is enhanced by the large nonresonant background.

Theoretical calculations of both the resonant and the nonresonant spectrum, the relative phase between the two, and the resulting signal spectrum, due to their coherent sum, are presented in Figs. 6(a)–6(b). The calculations are performed for a transform limited pulse and a pulse shaped by a 10-pixel (≈ 3 nm) π phase gate illuminating a $\text{Ba}(\text{NO}_3)_2$ sample. As is evident, applying a phase gate induces two peaks at the resonant spectrum, which are located at the phase gate edges (shifted by the Raman energy). In addition, the relative phase between the resonant and the nonresonant components varies rapidly across the phase gate [see Fig.

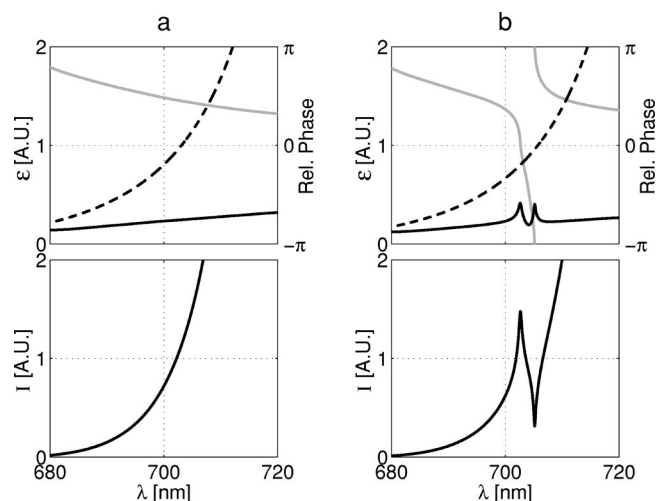


FIG. 6. The top images show the calculated CARS electric field as a function of frequency for the resonant signal (solid line) and the nonresonant background (dashed line) for $\text{Ba}(\text{NO}_3)_2$. Also shown is the relative phase between the two (gray line). The bottom images show the calculated resulting CARS spectrum. (a) Transform-limited pulse. (b) Phase-gate shaped pulse.

6(b)]. Destructive interference with the nonresonant background is induced at the long-wavelength edge of the phase gate, whereas constructive interference is induced at the short-wavelength edge. In the total signal, due to the interference of the two, a dip and a peak appear, corresponding to the two respective edges of the phase gate. The combined effect results in a narrow spectral structure on the measured spectrum. It is a direct consequence of the existence of a resonant level, where its location on the power spectrum is determined by the level's energy. In the following we exploit this effect to show an alternative mechanism for a Raman spectrum measurement.

B. Experimental results

In order to demonstrate this effect on the signal spectrum, we filtered the signal by a computer controlled monochromator, and measured the CARS signal power spectrum both with a transform limited and with a pulse shaped by a 10-pixel π phase gate. As predicted, when measuring the signal obtained from $\text{Ba}(\text{NO}_3)_2$ having a single resonant Raman level at 1048 cm^{-1} , sharp maximum followed by a minimum is exhibited for the shaped pulse [see Fig. 7(a)]. In a simple approach, the Raman level structure is extracted from the measured spectrum by considering the normalized spectral intensity variation of the CARS signal,

$$f(\Omega) = - \frac{I(\omega_g + \Omega - \Delta_g/2) - I(\omega_g + \Omega + \Delta_g/2)}{\int_{\omega_g + \Omega - \Delta_g/2}^{\omega_g + \Omega + \Delta_g/2} I dI}, \quad (10)$$

where ω_g is the central frequency of the phase gate. The normalization is required to compensate for the decrease in the nonresonant background towards higher energies. Figure 7(b) presents an analysis of the measured CARS spectrum for both a transform limited pulse and a shaped pulse, using Eq. (10). While no spectral information is observed with a transform limited pulse, when using a shaped pulse a sharp

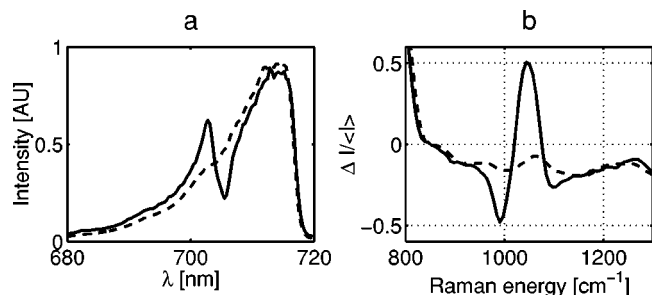


FIG. 7. Narrow probing by a phase gate shaped pulse. (a) CARS spectra from $\text{Ba}(\text{NO}_3)_2$ (resonant at 1048 cm^{-1}) for the transform limited pulse (dashed line) and phase gate shaped pulse (solid line). (b) Respective normalized vibrational energy levels as derived from the measured spectra by differentiating the relative intensity over the gate width according to Eq. (10), for the transform limited pulse (dashed line) and phase gate shaped pulse (solid line).

peak at 1048 cm^{-1} appears. The observed peak is accompanied by two dips, which are related to the simplicity of the analysis. Figure 8(a) presents the measured signal together with a theoretical calculation for toluene, which has a more complicated Raman spectrum. Three well-separated peaks are observed in the measured spectrum [see Fig. 8(b)], related to the Raman levels 788 , 1001 , and 1210 cm^{-1} . The asymmetry of the peak of 1001 cm^{-1} is due to the weak contribution from the 1028 cm^{-1} level. It is evident that the spectral information obtained by Eq. (10) is in good agreement with the theoretical calculation. The spectral resolution here is determined by convolution the lifetimes of the vibrational levels, the phase gate width (40 cm^{-1}), the shaper resolution (5 cm^{-1}), and the set monochromator resolution (10 cm^{-1}).

V. CONCLUSION

The results presented here show that single-pulse vibrational spectroscopy can be readily achieved using coherent control techniques and that these techniques can extend to the important fingerprint region. These techniques overcome two major difficulties usually associated with femtosecond CARS spectroscopy, namely, limited spectral resolution and strong background from nonresonant processes. By tailoring the spectral phase of an ultrashort pulse, we are able to control the interference between quantum processes induced by

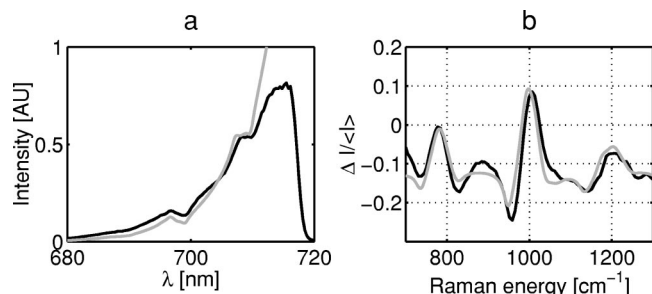


FIG. 8. (a) CARS spectra from toluene (resonant at 788 , 1001 , 1028 , and 1210 cm^{-1}), (black line) along with the calculation prediction (gray line). (b) Vibrational energy levels as derived from the measured spectra (black line) along with the calculation predictions (gray line).

the various spectral components of the pulse, leading either to selective population of given Raman levels or to the generation of narrow features in the CARS spectrum by all the populated Raman levels. By applying this principle we demonstrated high-resolution spectroscopy, two orders of magnitude better than the spectral bandwidth, in the vibrational energy range $700\text{--}1400\text{ cm}^{-1}$, i.e., most of the fingerprint region. By measuring a complex Raman spectrum of a molecule in this spectral region we have demonstrated the method to be robust and practical. To cover the fingerprint region, we have used $\sim 10\text{ fs}$ pulses that are readily available today from modelocked Ti:sapphire lasers. All the results presented were obtained with unamplified pulses directly from the laser oscillator and they were modeled exactly with a perturbative approach. This enables simple yet precise modelling of the nonlinear interaction, and tailoring of the pulse shape to the specific measured system.

Single-pulse CARS is particularly suitable for nonlinear microscopy applications. In contrast to conventional nonlinear CARS microscopy, which requires two synchronized tunable sources, single-pulse CARS only requires a single ultrashort laser at a fixed wavelength. The spectral measurements are performed by use of an electronically controlled spatial light modulator. Such a system is very conveniently coupled to a scanning optical microscope to obtain chemical information with high three-dimensional spatial resolution. Now that these techniques have been extended to the fingerprint region, CARS imaging can be applied to a multitude of organic chemicals with many exciting application in medical sciences and biology.

ACKNOWLEDGMENTS

Financial support by the Israel Science Foundation and by the Bundesministerium für Bildung und Forschung is gratefully acknowledged.

- ¹A. M. Weiner, D. E. Leaird, G. P. Wiederrecht, and K. A. Nelson, *J. Opt. Soc. Am. B* **8**, 1264 (1991).
- ²D. Meshulach and Y. Silberberg, *Phys. Rev. A* **60**, 1287 (1999).
- ³N. Dudovich, B. Dayan, S. M. Gallagher Faeder, and Y. Silberberg, *Phys. Rev. Lett.* **86**, 47 (2001).
- ⁴N. Dudovich, D. Oron, and Y. Silberberg, *Phys. Rev. Lett.* **12**, 123004 (2002).
- ⁵S. R. Judson and H. Rabitz, *Phys. Rev. Lett.* **68**, 1500 (1992).
- ⁶A. Assion, T. Baumert, M. Bergt, T. Brixner, B. Kiefer, V. Seyfried, M. Strehle, and G. Gerber, *Science* **282**, 919 (1998).
- ⁷R. Bartels, S. Backus, E. Zeek, L. Misoguti, G. Vdovin, I. P. Christov, M. M. Murnane, and H. C. Kapteyn, *Nature (London)* **406**, 164 (2000).
- ⁸T. C. Weinacht, J. Ahn, and P. H. Bucksbaum, *Nature (London)* **397**, 233 (1999).
- ⁹*Infrared and Raman Spectroscopy*, edited by B. Schrader (VCH, Weinheim, 1995).
- ¹⁰R. Leonhardt, W. Holzappel, W. Zinth, and W. Kaiser, *Chem. Phys. Lett.* **133**, 373 (1987).
- ¹¹D. Oron, N. Dudovich, D. Yelin, and Y. Silberberg, *Phys. Rev. A* **65**, 043408 (2002).
- ¹²D. Oron, N. Dudovich, D. Yelin, and Y. Silberberg, *Phys. Rev. Lett.* **88**, 063004 (2002).
- ¹³Y. X. Yan, L. T. Cheng, and K. A. Nelson, *Advances in Nonlinear Spectroscopy*, Vol. 16 in *Advances in Spectroscopy Series*, edited by R. J. H. Clark and R. E. Hester (Wiley, Chichester, 1988).
- ¹⁴N. Dudovich, D. Oron, and Y. Silberberg, *Nature (London)* **418**, 512 (2002).

- ¹⁵J. X. Cheng, A. Volkmer, L. D. Book, and X. S. Xie, *J. Phys. Chem. B* **105**, 1277 (2001).
- ¹⁶D. Oron, N. Dudovich, and Y. Silberberg, *Phys. Rev. Lett.* **89**, 273001 (2002).
- ¹⁷D. Oron, N. Dudovich, and Y. Silberberg, *Phys. Rev. Lett.* (to be published).
- ¹⁸G. Stobrawa, M. Hacker, T. Feurer, D. Zeidler, M. Motzkus, and F. Reichel, *Appl. Phys. B: Lasers Opt.* **72**, 627 (2001).
- ¹⁹A. M. Weiner, *Rev. Sci. Instrum.* **71**, 1929 (2000).
- ²⁰The modulation amplitude was chosen as approximately half of the first zero of the Bessel function J_0 , leading to the largest modulation of the population (from the maximum value obtained by a transform limited pulse, down to zero).